Machine Learning Models for Water Level Prediction in Rapid Urban Streams: Case of Mburicaó, Asunción, Paraguay

Mathias Aguilar, Héctor Velázquez, Diego H. Stalder, Andrés Wehrle, Jazmín Ojeda
Facultad de Ingeniería, Universidad Nacional de Asunción
San Lorenzo, Paraguay
Emails: {maguilar, hvelazquez, jazmin.ojeda}@fiuna.edu.py, {dstalder, awehrle}@ing.una.py

Leonardo B.L. Santos
National Center for Monitoring and Early Warning of Natural Disasters (Cemaden)
São José dos Campos, SP, Brazil
santoslbl@gmail.com

***Abstract*—Urban streams in rapidly growing cities are increasingly susceptible to sudden rises in water levels during intense precipitation events due to the lack of public investment or extreme natural events. This work investigates water level peaks and significant flooding events in the Mburicaó stream in Asunción, Paraguay. We develop two predictive models using ten-minute interval data from three weather stations: a support vector machine classifier (SVM) to detect threshold-exceeding events and a multilinear regression model to estimate peak water levels. We employ mutual information analysis combined with cross-correlation between stream level and lagged precipitation to inform the selection of predictive input features. Our results indicate that with rainfall data from 40 minutes before the peak of a flood event, the regression model obtains a coefficient of determination (R^2) of 0.8209, an RMSE of 0.3509 meters, and a MAPE of 31.27%. While the classification model, with a 50-minute prediction horizon, targeting occurrences with peaks larger than 1.0 meters, achieves an F1-score of 0.66 with 85% recall and 54% precision. The classification performance still shows potential for improvement, especially in lowering false positives by having longer time series of data or considering hydrological models. These models could be the basis of early warning systems in data-scarce urban environments, offering a practical tool for risk mitigation in Paraguay.**

***Index Terms*—River Level Forecasting**

I. Introduction

Efforts to address flood risks in Asunción have involved urban planning strategies like rainwater harvesting to decrease runoff volume and peak flow [1]. For operational flood response, the ability to forecast river level changes in real time is important. Short-term prediction tools can assist early warning systems and enable local authorities and communities to prepare or respond more effectively.

Representing quickly evolving cities and the nonlinear dynamics frequently seen in urban hydrology is a major problem. Commonly utilized in alarm systems, hydrological models are based on physical principles and need significant computational resources and rigorous calibration, which limits their use in urban environments, particularly when real-time execution is required [2], [3].

Machine learning (ML) methods provide a flexible option. Several techniques, such as SVM, artificial neural networks (ANN), adaptive neuro-fuzzy inference systems (ANFIS), and ensemble decision trees have been used in river and lake level forecasting [4], [5], [6], [7], [8]. Some studies have incorporated these approaches into early warning frameworks [9], [10], and comparative analyses indicate that data-driven models can perform on par with traditional statistical approaches in certain contexts [11], [12].

In this context, our study explores a practical, data-informed framework for real-time flood prediction in the Mburicao stream in Asuncion, Paraguay. We utilize ten-minute interval precipitation and stream level data from three meteorological stations to create two predictive models: (i) a LR model aimed at estimating peak stream levels, and (ii) a SVM classifier designed to determine if an event surpasses a specified critical threshold. We combine the mutual information (MI) and cross-correlation analysis with temporal lags, aligning the peaks level with the rainfall and the stream's concentration time.

This paper is structured as follows: Section II describes the dataset and study area, Section III details the feature engineering process, Section IV presents the LR model for peak water level prediction, Section V introduces the SVM-based event classification framework, and Section VI discusses the literature about urban flash flood forecasting. Finally, Section VII discusses the implications of our findings and future directions—including integration with hydrological models—to enhance predictive accuracy for urban flood early warning systems.

979-8-3503-4807-1/23/$31.00 ©2023 IEEE

II. Dataset

This study is based on environmental data collected from three meteorological stations located in the metropolitan area of Asunción, Paraguay (see Figure 1): San Ignacio de Loyola (SIL), Secretaría Nacional de Deporte (SND), and Aeropuerto Internacional Silvio Pettirossi (AISP). Table I summarizes the coordinates of the sensors' locations. Each station records rainfall at ten-minute intervals, while SIL uniquely includes water level measurements from the Mburicao stream.

We analyzed two distinct temporal subsets:

(Set1) July-August 2021 (all stations)

(Set 2) July 2021-May 2022 (SIL data only, including both water level and rainfall measurements)

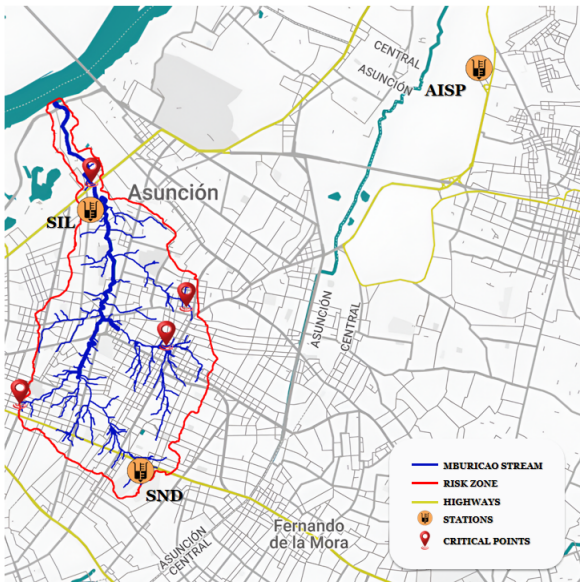

Fig. 1: Map showing the location of meteorological stations and critical points along the Mburicao stream. The watershed is outlined in red, and the basin is indicated in blue.

TABLE I: Summary of measurement stations.

Station	City	(Lat., Long.)	Variables
SIL	Asunción	-25.27, -57.59	Precipitation, Stream level
SND	Asunción	-25.32, -57.58	Precipitation
AISP	Luque	-25.24, -57.51	Precipitation

We found 56 instances in the dataset, which spans 11 months, where rainfall conditions—from light showers to a few severe storm events—led to an elevation in the stream level. The research period's temporal fluctuations in rainfall and stream levels (the target variable) are depicted in Figure 2. In order to preprocess the data, we used the timestamp to align measurements across stations. Set 2 had more flood events, so we concentrated our modeling efforts there, even if Set 1 assisted in assessing precipitation-to-peak lag times.

III. Feature Engineering

The quality and relevance of input features play a significant role in the performance of machine learning models,

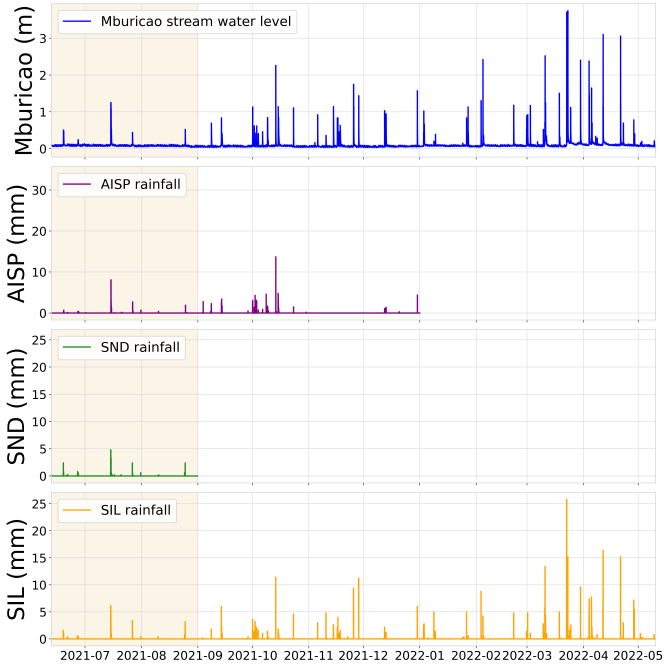

Fig. 2: Time series of rainfall and water level measurements at different stations.

particularly in time-sensitive applications like real-time flood forecasting. Our dataset has rainfall measurements from three stations to develop predictive features that reflect the relationship between precipitation and changes in stream levels. Figure 3 shows an event without high risk that took place on July 27, 2021, when the stream level reached about 0.45 m around midnight. The figure shows a rainfall recorded at the SIL station preceding a sharp increase in stream level.

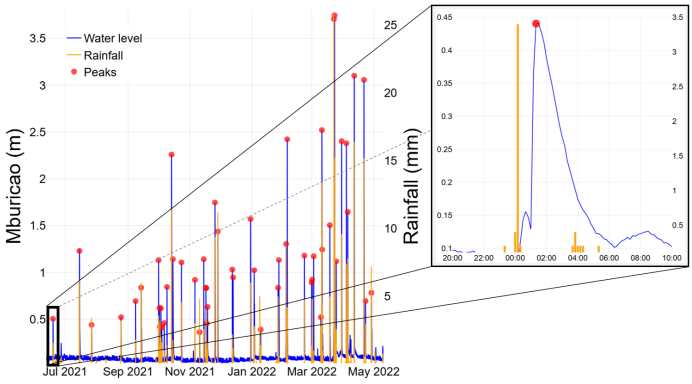

Fig. 3: Time series of stream level and rainfall for the event of July 27, 2021. The inset highlights the rapid increase in stream level following local precipitation measured at the SIL station.

A. Feature Selection Strategy

Two methods are examined to quantify the lag with maximices the correlations between rainfall and stream response and enhancing model interpretability:

- Mutual Information (MI): This method assesses the relationship between each feature and the target variable, organizing features according to their estimated contribution. The mutual information is calculated as:

$$(X;Y) = \sum_{x\in X}\sum_{y\in Y} p(x,y)\log\left(\frac{p(x,y)}{p(x)p(y)}\right) \quad (1)$$

- **Cross-Correlation**: This method evaluates the timing relationship between rainfall and stream level data.

Figure 4 presents the MI scores for a selection of rainfall features, while Figure 5 shows how cross-correlation assists in determining which lags provide useful information for predicting hydrological response. The AISP station is not located within the Mburicao basin, which explains the greater lag and lower correlation observed Figure 4 presents the

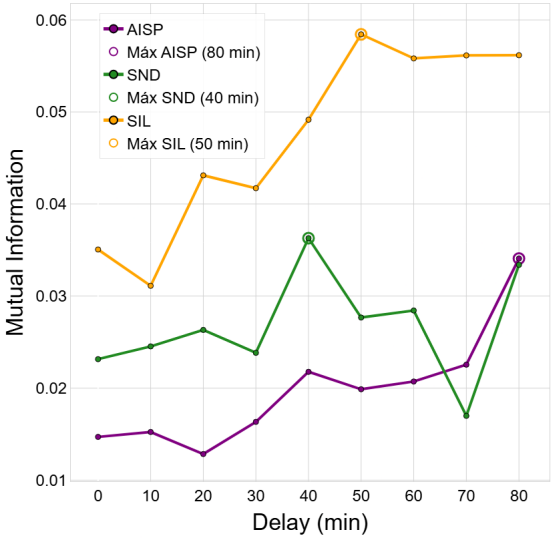

Fig. 4: Mutual information analysis of rainfall-derived features and the target variable.

mutual information between each rainfall-derived feature and the target variable (peak stream level), highlighting the role of each time lag in the prediction, with a notable peak occurring 50 minutes prior.

In a similar manner, the cross-correlation plot in Figure 5 shows that the strongest correlations between rainfall and stream response take place within the first 40 to 50 minutes before the event. Following this period, the correlation diminishes significantly. According to these analyses, the temporal aggregation was restricted to a maximum of 80 minutes before the peak (t_8) to prevent the inclusion of features with minimal informational value or erratic behavior, while maintaining an adequate time frame for early prediction.

B. Temporal Aggregation of Rainfall

To examine the effect of rainfall on stream level peaks, two types of features were derived from meteorological data:

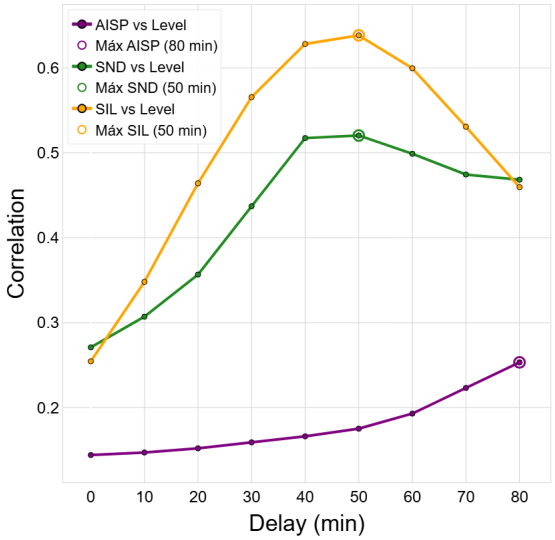

Fig. 5: Pearson Cross-correlation between rainfall time series and stream level response.

instantaneous rainfall $R(t)$ and accumulated rainfall R_i^{acc}. Accumulations were determined using sliding windows of varying lengths, covering the period from 80 minutes before the peak event (denoted as t_8) up to a specific prediction horizon $t_i = t_0 - 10H$, where H is the number of minutes before the reference timestamp t_0.These features were computed independently for each meteorological station.

Each accumulation window is defined as:

$$R_i^{\text{acc}} = \sum_{t=t_8}^{t_i} R(t), \quad (2)$$

where $R(t)$ represents the rainfall intensity at time t, and the summation spans the corresponding window ending at the prediction horizon. This formulation allows the models to integrate recent rainfall intensities and accumulated rain to capture the temporal dynamics of the stream's hydrological response.

IV. Regression Model for Peak Prediction

This section presents the regression model to predict the peak of each event. Figure 6 illustrates the features selected for each model. For a given prediction horizon H, each model adopts a specific configuration based on the time interval to the peak t_0. The accumulation window length L indicates the number of inputs of rainfall data considered in the model. By using features derived from various combinations of L and H, we examine how rainfall patterns relate to streamflow peaks, enabling the analysis of different lead times and accumulation behaviors.

On each model, Figure 6 displays which features are used. For a given prediction horizon H each model has a particular configuration, considering the time interval between the peak

t_0 , we have Ta length L of each accumulation window indicates the number of minutes of rainfall that are considered. By collecting features with different L and H, we investigate the relationship between rainfall and streamflow peaks, allowing us to investigate different lead times and accumulation patterns.

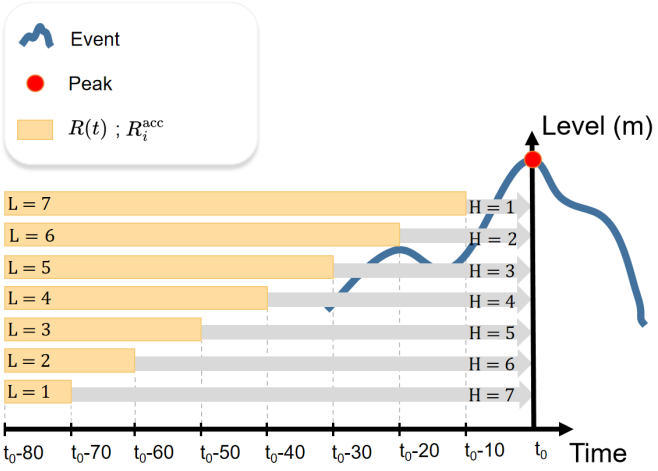

Fig. 6: Schematic representation of rainfall accumulation features for regression modeling. Each orange bar corresponds to an accumulation window of length L, ending at a prediction horizon H before the streamflow peak at t_0.

A. Linear Regression

The prediction of peak stream level is conducted using a multiple LR model, where the input feature vector $\mathbf{X} \in \mathbb{R}^n$ consists of both instantaneous rainfall values $R(t)$ and accumulated precipitation R_i^{acc}. Instantaneous features indicate short-term rainfall intensity at certain timestamps, whereas accumulated features illustrate wider precipitation patterns over specified intervals of length L, concluding at the prediction horizon H prior to the peak time t_0.

The regression model is presented as follows:

$$\hat{y} = \beta_0 + \sum_{j=8}^{L} \beta_j R(t_j) + \sum_{k=8}^{L} \alpha_k R_k^{\text{acc}}(t_k), \tag{3}$$

where β_0 indicates the intercept, the first summation term consists of instantaneous rainfall values $R(t_j)$ at particular time steps t_j before the event, each multiplied by a coefficient β_j. The coefficients measure how short-term rainfall intensity at minute t_j affects the overall peak level. The second summation term includes accumulated rainfall values $R_k^{\text{acc}}(t_k)$, which represent the total precipitation over a window of length L that concludes at time t_k. Each accumulated feature is linked to a coefficient α_k, indicating the extent of influence that specific rainfall interval has on the peak level.

By distinguishing β_j (for instantaneous values) and α_k (for accumulated values), the model is able to separately weigh the short-term and longer-term contributions of rainfall, offering greater interpretability across different temporal scales. This structure enables exploration of how different combinations of recent and earlier precipitation contribute to the streamflow peak prediction.

Model performance was evaluated using three standard metrics:

- R^2: the coefficient of determination, showing the proportion of variance accounted for by the model.
- RMSE: root mean squared error, measuring the average size of prediction errors.
- MAPE: mean absolute percentage error, providing a straightforward measure of prediction accuracy in relation to observed values.

B. Experimental Results

We assessed the practicality of predicting peak stream levels by training over various H. Each value of $H \in \{1, 2, \ldots, 7\}$ is associated with a lead time in minutes prior to the observed peak time t_0.

The implementation uses the `LinearRegression` class from the `scikit-learn` library. To identify a suitable set of features for peak prediction, we performed a comprehensive grid search across all the combinations (until t_8) of instantaneous $R(t_j)$ and accumulated $R_k^{\text{acc}}(t_k)$ rainfall features. For each prediction horizon H, various subsets of features were assessed through 5-fold cross-validation. The selection criterion focused on reducing validation error, primarily assessed through the Root Mean Squared Error (RMSE) and complemented by other metrics like R^2 and MAPE.

TABLE II: LR results across different prediction horizons.

H	Selected Features	R^2	RMSE (m)	MAPE (%)
1 (10min)	$R(t_7)$, $R(t_8)$, $R_{t_1}^{acc}$, $R_{t_7}^{acc}$	0.8412	0.3304	27.61
2 (20min)	$R(t_5)$, $R(t_7)$, $R_{t_2}^{acc}$, $R_{t_7}^{acc}$	0.8443	0.3272	28.07
3 (30min)	$R(t_5)$, $R(t_7)$, $R_{t_3}^{acc}$, $R_{t_7}^{acc}$	0.8470	0.3243	28.19
4 (40min)	$R(t_4)$, $R(t_6)$, $R_{t_6}^{acc}$, $R_{t_7}^{acc}$	0.8209	0.3509	31.27
5 (50min)	$R(t_5)$	0.6139	0.5152	36.72
6 (60min)	$R(t_7)$, $R_{t_6}^{acc}$	0.0478	0.8090	73.72
7 (70min)	$R(t_7)$	0.0194	0.8210	76.39

Table II summarizes the performance of the multiple LR model across different prediction horizons. The results indicate that configurations with $H \in \{1, 2, 3, 4\}$, which correspond to horizons between 10 and 40 minutes, tend to have higher R^2 values and lower RMSE and MAPE scores. This indicates that rainfall happening just before the peak has a more direct impact on stream level increases, and thus provides a clearer predictive signal. Models that utilize larger H values (i.e., longer horizons) often demonstrate lower performance, possibly because earlier rainfall becomes less relevant or due to the presence of additional variability.

Based on this analysis, we chose the configuration associated with $H = 4$, indicating a prediction horizon of 40 minutes

prior to the streamflow peak. The feature set that performed well for this case included four variables: instantaneous rainfall at 40 and 60 minutes prior to the peak ($R(t_4), R(t_6)$), and accumulated rainfall over the 60 and 70 minute windows ($R^{acc}_{t_4}, R^{acc}_{t_7}$).

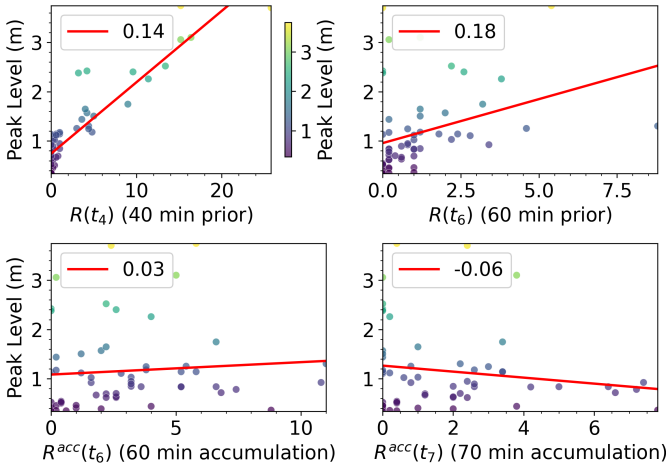

Fig. 7: Simple LR between each rainfall feature (mm) and the observed peak stream level (m). Each subplot shows the raw scatter plot and fitted regression line, using unscaled feature values. The color scale indicates the magnitude of the peak level.

Figure 7 confirms the simple linear relationships between each rainfall feature and the observed peak stream levels. Among all features, the instantaneous rainfall at 40 minutes prior $R(t_4)$ shows the strongest positive linear relationship with peak level, while accumulated rainfall at 70 minutes prior $R(t_7)$ displays a weaker and less consistent pattern. This analysis shows a connection between early forecasting potential and predictive reliability.

V. Event Classification Model (SVM)

Beyond estimating streamflow magnitudes, it is equally important to determine whether an incoming event should trigger a flood alert. In this section, we describe a binary classification approach using a SVM to predict whether the observed stream level will exceed a predefined threshold.

A. Problem Definition

The classification task involves a binary target variable $y \in \{0, 1\}$, where $y = 1$ signifies that the peak water level during the event meets or surpasses a critical threshold h_{crit}, and $y = 0$ indicates that it does not. The model receives a feature vector created from rainfall data collected decribed in previouse section.

We assess model robustness by examining different severity levels and the associated thresholds.

$$h_{\text{crit}} \in \{0.5\,\text{m},\ 1.0\,\text{m},\ 1.5\,\text{m},\ 2.0\,\text{m}\}$$

Every threshold establishes a unique classification situation. The experiments discussed here concentrate on $h_{\text{crit}} = 1.0\,\text{m}$, a typical operational threshold often applied in flood monitoring. These definitions are illustrated in Figure 8, which outlines the temporal dynamics that guide both labeling and input feature construction. This representation helps visualize the relationship between rainfall timing and classification output, which is particularly relevant in early warning scenarios.

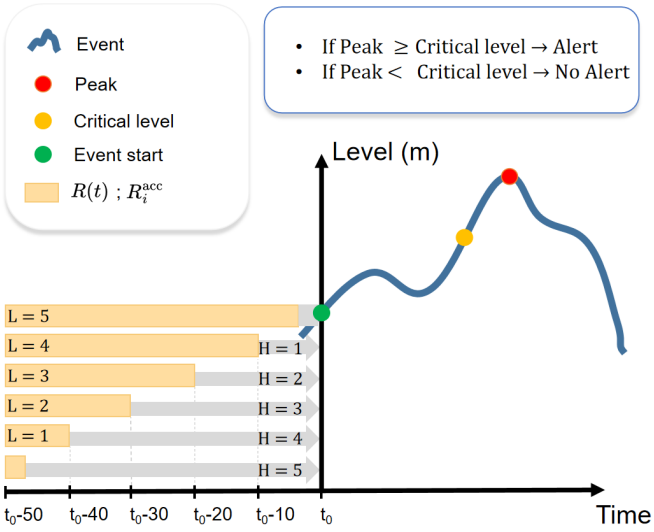

Fig. 8: Illustration of an event classification setup, including the event start threshold, the critical peak level h_{crit}, and the rainfall accumulation window used to construct features for the classifier.

B. SVM Formulation

The SVM classifier transforms the input features into a higher-dimensional space through a nonlinear process and identifies a decision boundary that aims to increase the margin between classes. The optimization problem for the soft-margin SVM with an RBF kernel can be expressed as follows:

$$\min_{\mathbf{w},b,\xi} \frac{1}{2}\|\mathbf{w}\|^2 + C\sum_{i=1}^{n}\xi_i \tag{4}$$

subject to:

$$y_i(\mathbf{w}^\top \phi(\mathbf{x}_i) + b) \geq 1 - \xi_i, \quad \xi_i \geq 0, \tag{5}$$

where $\phi(\cdot)$ indicates the feature mapping, C denotes the penalty parameter, and ξ_i are slack variables that permit certain misclassifications. The SVM classifier was set up using the `SVC` class with a radial basis function (RBF) kernel and balanced class weights to address label imbalance. Models were implemented with the `SVC` class from the `scikit-learn` library, using cross-validation for hyperparameter tuning.

C. Experimental Results

The evaluation of model performance was conducted using four classification metrics. Precision refers to the ratio of true positive cases to the total number of predicted positive cases. Recall refers to the proportion of actual positive cases that are

accurately predicted. The F1 score is the harmonic mean of precision and recall, serving as a balanced indicator of performance. False negatives refer to the instances of missed critical events, which hold significance in early warning systems.

We explored how classification performance changes based on the prediction horizon, which ranges from 50 to 10 minutes prior to the streamflow peak. The classifier underwent testing with feature sets obtained from rainfall accumulation windows, which were chosen through grid search for each configuration.

Results for the 1.0 m threshold are summarized in Table III indicates that shorter prediction horizons lead to a more balanced relationship between precision and recall.

TABLE III: SVM classification performance and selected features at threshold $h_{\text{crit}} = 1.0\,\text{m}$.

H	Selected Features	F1-Score	Precision	Recall
1	$R(t_2), R(t_3), R(t_5), R^{\text{acc}}_{t_1}$	0.8235	0.8400	0.8077
2	$R(t_2), R(t_3), R(t_4), R(t_5), R^{\text{acc}}_{t_5}$	0.7755	0.8261	0.7308
3	$R(t_3), R(t_5)$	0.6000	0.8571	0.4615
4	$R(t_4), R(t_5), R^{\text{acc}}_{t_5}$	0.6364	0.5250	0.8077
5	$R(t_5)$	0.6567	0.5366	0.8462

According to the classification results in Table III, we chose the configuration with $H = 5$, which relates to a prediction horizon of 10 minutes prior to the streamflow peak. While its F1-score is a bit lower than that of $H = 1$, this configuration reaches the highest recall (0.8462) and the fewest false negatives. In early warning systems, reducing missed critical events is an important goal, since false negatives indicate undetected flood risks. The chosen model offers a balance between prompt alerts and effective detection performance, making it appropriate for real-time use in operational situations.

TABLE IV: Observed and predicted outcomes for the classification model ($h_{\text{crit}} = 1.0\,\text{m}$, $H = 5$).

		Predicted	
		No Event	Event
Observed	No Event	13	19
	Event	4	22

Table IV shows the confusion matrix for $H = 5$, its second indicates that the model identified 22 out of 26 critical events, resulting in 4 false negatives, indicating its ability to detect high-risk cases. However, the model generated 19 false positives, which are not desirable, these false alarms might be reasonable in situations where early warnings are valued more than precise accuracy, especially when the consequences of overlooking a flood event are greater than the trouble caused by a false alert.

Figure 9 shows the predicted outcomes over time for events evaluated with a threshold of 1.0 m and a window of $H = 5$. Each peak that is larger than the threshold is identified, differentiating between accurately predicted critical events and those that the model did not recognize. The figure indicates that false negatives tend to occur more often with medium-sized events. These cases indicate that borderline or less intense rainfall episodes are more difficult to predict.

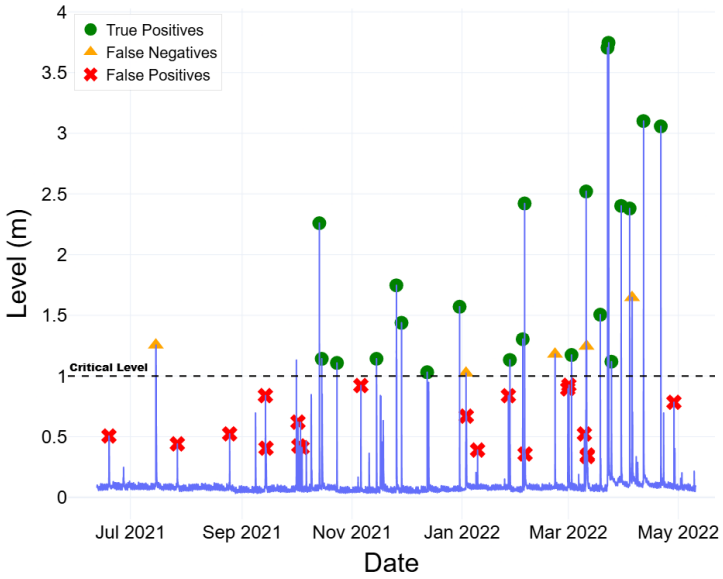

Fig. 9: Predicted critical events using the SVM classifier at $h_{\text{crit}} = 1.0\,\text{m}$ and $H = 5$ (50min). Green circles indicate correctly predicted critical events (true positives), yellow triangles mark missed detections (false negatives), and red crosses represent false alarms (false positives)

The increase in false negatives for larger H values suggests that using older rainfall data could introduce noise rather than improve signal detection. This behavior holds significance for real-time applications, as missed alerts can affect the system's reliability in high-risk situations. The SVM classifier is easy to implement and demonstrates consistent performance when trained on certain rainfall intervals. To enhance performance, particularly in minimizing false positives, future efforts might consider decision threshold calibration, temporal ensemble strategies, or the inclusion of hydrological state variables to better refine prediction confidence. The performance can be modified to emphasize recall or precision according to the operational requirements of the flood alert system. Future work will explore hybrid classifiers or ensemble methods to improve sensitivity to rare but important events.

VI. Discussion

Flood prediction models are crucial for risk management and evacuation planning. Current prediction models are based on simplified assumptions and data, most of which attempt to replicate mathematical representations of physical processes and watershed behavior, which are highly specific and complex [13], [14].

The approach to real-time flood prediction is broad. For example, a study conducted in Korea used scenarios with logistic regression models to generate a flood probability discriminant for each grid cell comprising the study area and

predict flood extent based on the amount of rainfall-caused runoff. To this end, 100 rainfall probability scenarios were created by combining return period, duration, and temporal distribution using past observational rainfall data. Databases of the rainfall-runoff-flood relationship were constructed for each scenario using hydrodynamic and hydrological models. A logistic regression-based flood probability discriminant was generated for each grid using whether the grid was flooded (1 or 0) as a proxy for the runoff amount in the database [15].

Machine learning (ML) models include sophisticated data-driven methods and are used for their low computational cost and flexibility to represent flood nonlinearities using only historical data without requiring an understanding of underlying physical processes. In this regard, numerous ML models have demonstrated greater accuracy than conventional statistical methods for predicting floods in both the short and medium term. Furthermore, ML performance could be improved by combining it with physical models to generate more robust and efficient models capable of adaptively learning complex flood systems [13].

This study employs a combination of predictive models using accumulated precipitation data as input. A LR model for estimating maximum levels, and SVM model allows classifying flood events if they exceed a threshold defined at stations located in the urban basin of Arroyo Mburicao.

Similar work was carried out in Shenzhen, China, where a precipitation threshold was used to classify flood and non-flood events, based on machine learning (ML) approaches. Several rainfall threshold lines were determined, projected onto a plane spanned by two principal components, providing a binary outcome (flood or no flood). Compared to the conventional critical rainfall curve, the proposed models (decision trees, discriminant analysis (DA), support vector machines (SVM), K-nearest neighbor, Bagged Trees, and Subspace Ensembles) allowed classifying flood and non-flood events by different combinations of multi-resolution rainfall intensities, increasing accuracy to 96.5% and reducing the false alert rate to 25%. Compared to the conventional model, the critical accuracy indices and true positive rate (TPR) were between 5% and 15% higher in ML models [14].

Furthermore, another study conducted in Pakistan to develop machine learning-based urban flood risk prediction models suggests that when comparing the performance of several models employing ML techniques, the SVM performs best in accurately predicting flood occurrences. The dataset covered four features: precipitation, temperature, monthly discharge, and flood occurrence. The results indicated that SVM achieved the highest accuracy among the analyzed algorithms (KNN, NB, ANN, RF), with a value of 82.40% [16].

On the other hand, other works propose the use of hybrid models for urban flood susceptibility mapping, employing support vector regression (SVR) integrated with a combination of wavelet transform and metaheuristic optimization algorithms. The data used included distance from the channel, distance from the river, bend number, slope, elevation, and precipitation. The spatial analysis highlights the importance of conditioning factors, since in the analysis performed, precipitation was the least important factor due to its low spatial variability for the study area [17].

From all the above, it is notable that ML methods contribute to the advancement of prediction systems, as they offer better performance and cost-effective solutions. However, ML methods have important characteristics that must be considered. First, their quality depends on training, through which the system learns the target task based on previous data. The second aspect is the capability of each ML algorithm, which can vary across different types of tasks, as it indicates how well the trained system can predict cases for which it was not trained, i.e., whether it can predict beyond the range of the training dataset. For example, ML methods used for short-term water level prediction differ significantly from those used for long-term streamflow prediction [18]. Finally, spatial flood prediction to estimate or identify the location of floods introduces other factors that increase the complexity of the analysis.

VII. Conclusion

This study develop a data-driven approach to predicting peak water levels and identifying significant streamflow occurrences in the Mburicaó urban basin. Two predictive models were implement by analyzing rainfall data from three weather stations: an SVM classifier to determine whether an event exceeds predetermined criteria and an LR model to estimate peak amounts.

The LR model reached a $R^2 = 0.8470$, with a root mean squared error (RMSE) of about 0.32 meters and a mean absolute percentage error (MAPE) close to 28% when analyzing rainfall windows of 10 to 30 minutes before peak events. The results show that simple models can provide useful short-term estimates of stream response in urban catchments.

The SVM model aimed to predict when a critical level of 1.0 meters would be exceeded for event classification. The configuration chosen with a prediction horizon of 10 minutes before peak ($H = 5$) resulted in an F1-score of 0.66, along with a precision of 0.54 and a recall of 0.85. This model exhibits a trade-off and naturally permits a manageable number of false positives. Although it is acknowledged that there may be sporadic false alarms, this behavior is frequently regarded as appropriate in early warning systems where the focus is on optimizing event detection.

A limitation encountered in this study is the absence of an operational real-time monitoring infrastructure within the basin. Radar sensors and rain gauges were installed earlier, but they are not functioning at the moment. Current initiatives focus on bringing these instruments back into use. At the same time, working together with initiatives like [1] is recommended to enhance level-flow characterization and to set up new measurement sites in important subregions of the basin.

The models developed here could be the base to create early warning systems in metropolitan regions of Asunción and their incorporation into a real-time monitoring platform could help local communities and municipal agencies receive targeted and

timely alerts. This method combines can asimilate information in high-frequency data using lightweight models to build a scalable framework for urban flood resilience.

ACKNOWLEDGMENT

Authors acknowledge the financial support given the Engineering Faculty (FIUNA) and the data provided Prof. Andres Wehrle, JO and DHS acknowledges the FEEI-PROCIENCIA-CONACYT-SISNI. This study was financed in part by the CNPq (Brazil) Project 446053/2023-6

REFERENCES

[1] A. Thiessen-Anttila, M. Castier, and P. Barreto, "Simulating the effect of rainwater harvesting on flood mitigation: the case of asunción, paraguay," *Natural Hazards*, vol. 121, pp. 4335–4358, 10 2024.

[2] G. K. Devia, B. Ganasri, and G. Dwarakish, "A review on hydrological models," *Aquatic Procedia*, vol. 4, pp. 1001–1007, 2015, iNTERNATIONAL CONFERENCE ON WATER RESOURCES, COASTAL AND OCEAN ENGINEERING (ICWRCOE'15). [Online]. Available: https://www.sciencedirect.com/science/article/pii/S2214241X15001273

[3] J. Hou, N. Zhou, G. Chen, M. Huang, and G. Bai, "Rapid forecasting of urban flood inundation using multiple machine learning models," *Natural Hazards*, vol. 108, no. 2, pp. 2335–2356, Sep 2021. [Online]. Available: https://doi.org/10.1007/s11069-021-04782-x

[4] W. J. Wee, N. B. Zaini, A. N. Ahmed, and A. El-Shafie, "A review of models for water level forecasting based on machine learning," *Earth Science Informatics*, vol. 14, no. 4, pp. 1707–1728, Dec 2021. [Online]. Available: https://doi.org/10.1007/s12145-021-00664-9

[5] A. N. Ahmed, A. Yafouz, A. H. Birima, O. Kisi, Y. F. Huang, M. Sherif, A. Sefelnasr, and A. El-Shafie, "Water level prediction using various machine learning algorithms: a case study of durian tunggal river, malaysia," *Engineering Applications of Computational Fluid Mechanics*, vol. 16, no. 1, pp. 422–440, 2022. [Online]. Available: https://doi.org/10.1080/19942060.2021.2019128

[6] S. S. Rudolf Scitovski, Siniša Maričić, "Short-term and long-term water level prediction at one river measurement location," *Croatian Operational Research Review*, vol. 3, 2012. [Online]. Available: https://hrcak.srce.hr/file/142442

[7] M. Ehteram, A. Ferdowsi, M. Faramarzpour, A. M. S. Al-Janabi, N. Al-Ansari, N. D. Bokde, and Z. M. Yaseen, "Hybridization of artificial intelligence models with nature inspired optimization algorithms for lake water level prediction and uncertainty analysis," *Alexandria Engineering Journal*, vol. 60, no. 2, pp. 2193–2208, 2021. [Online]. Available: https://www.sciencedirect.com/science/article/pii/S1110016820306840

[8] V.-H. Nhu, H. Shahabi, E. Nohani, A. Shirzadi, N. Al-Ansari, S. Bahrami, S. Miraki, M. Geertsema, and H. Nguyen, "Daily water level prediction of zrebar lake (iran): A comparison between m5p, random forest, random tree and reduced error pruning trees algorithms," *ISPRS International Journal of Geo-Information*, vol. 9, no. 8, 2020. [Online]. Available: https://www.mdpi.com/2220-9964/9/8/479

[9] J. A. J. P. Soares, L. C. S. M. Ozelim, L. Bacelar, D. B. Ribeiro, S. Stephany, and L. B. L. Santos, "Ml4ff: A machine-learning framework for flash flood forecasting applied to a brazilian watershed," *Journal of Hydrology*, vol. 652, p. 132674, 2025. [Online]. Available: https://www.mindat.org/reference.php?id=17914228

[10] A. Faruq, S. S. Abdullah, A. Marto, M. A. A. Bakar, Samin, and A. Mubin, "River water level forecasting for flood warning system using deep learning long short-term memory network," *IOP Conference Series: Materials Science and Engineering*, vol. 821, no. 1, p. 012026, apr 2020. [Online]. Available: https://dx.doi.org/10.1088/1757-899X/821/1/012026

[11] N. Imam Suprayogi1, Joleha2, "Applying adaptive neuro fuzzy inference system approach to river level forecasting," 2011. [Online]. Available: https://ejournal.uin-suska.ac.id/index.php/SNTIKI/article/view/2964

[12] J. Duque, L. B. d. L. Santos, R. Santos, R. Oyarzabal, and J. Arteaga, "Nonlinear hydrological time series modeling to forecast river level dynamics in the rio negro uruguay basin," *Chaos*, vol. 34, no. 5, p. 053132, 2024. [Online]. Available: https://pubmed.ncbi.nlm.nih.gov/38780437/

[13] M. Khan, A. U. Khan, B. Ullah, and S. Khan, "Developing a machine learning-based flood risk prediction model for the indus basin in pakistan," *Water Practice and Technology*, vol. 19, no. 6, pp. 2213–2225, 2024. [Online]. Available: https://iwaponline.com/wpt/article/19/6/2213/102848/Developing-a-machine-learning-based-flood-risk

[14] Y. Zhang, Z. Li, Y. Wang, Y. Wang, and Q. Zhang, "Urban flood prediction under heavy precipitation using machine learning models," *Journal of Hydrology*, vol. 586, p. 124956, 2020. [Online]. Available: https://www.sciencedirect.com/science/article/pii/S0309170819311601

[15] D. Kim, H. Kim, J. Lee, H. Lee, and S. Kim, "Scenario-based real-time flood prediction with logistic regression," *Water*, vol. 13, no. 9, p. 1191, 2021. [Online]. Available: https://www.mdpi.com/2073-4441/13/9/1191

[16] M. Khan, A. U. Khan, B. Ullah, and S. Khan, "Developing a machine learning-based flood risk prediction model for the indus basin in pakistan," *Water Practice and Technology*, vol. 19, no. 6, pp. 2213–2225, 2024. [Online]. Available: https://iwaponline.com/wpt/article/19/6/2213/102848/Developing-a-machine-learning-based-flood-risk

[17] O. Rahmati, H. Darabi, M. Panahi, Z. Kalantari, S. A. Naghibi, C. S. S. Ferreira, A. Kornejady, Z. Karimidastenaei, F. Mohammadi, S. Stefanidis, D. T. Bui, and A. T. Haghighi, "Development of novel hybridized models for urban flood susceptibility mapping," *Scientific Reports*, vol. 10, p. 12937, 2020. [Online]. Available: https://www.nature.com/articles/s41598-020-69703-7

[18] A. Mosavi, P. Ozturk, and K.-W. Chau, "Flood prediction using machine learning models: Literature review," *Water*, vol. 10, no. 11, p. 1536, 2018. [Online]. Available: https://www.mdpi.com/2073-4441/10/11/1536